coatings

MDPI

Article

MAPLE Deposition of Binary and Ternary Organic Bulk Heterojunctions Based on Zinc Phthalocyanine

Marcela Socol [1,*], Nicoleta Preda [1,*], Gabriela Petre [1,2], Andreea Costas [1], Oana Rasoga [1], Gianina Popescu-Pelin [3], Andreea Mihailescu [3], Anca Stanculescu [1] and Gabriel Socol [3]

1 National Institute of Material Physics, 405A Atomistilor Street, P.O. Box MG-7, 077125 Magurele, Romania; gabriela.petre@infim.ro (G.P.); andreea.costas@infim.ro (A.C.); oana@infim.ro (O.R.); sanca@infim.ro (A.S.)
2 Faculty of Physics, University of Bucharest, 405 Atomistilor Street, P.O. Box MG-11, 077125 Magurele, Romania
3 National Institute for Lasers, Plasma and Radiation Physics, 409 Atomistilor Street, P.O. Box MG-36, 077125 Magurele, Romania; gianina.popescu@inflpr.ro (G.P.-P.); andreea.mihailescu@inflpr.ro (A.M.); gabriel.socol@inflpr.ro (G.S.)
* Correspondence: marcela.socol@infim.ro (M.S.); nicol@infim.ro (N.P.)

Received: 21 September 2020; Accepted: 2 October 2020; Published: 4 October 2020

Abstract: Organic bulk heterojunctions (BHJ) based on zinc phthalocyanine (ZnPc), fullerene compounds (C60 fullerene and [6,6]-phenyl C71 butyric acid methyl ester (PC70BM)), and 5,6,11,12-tetraphenylnaphthacene (rubrene) were fabricated through the matrix-assisted pulsed-laser evaporation (MAPLE) technique. Thus, ZnPc:C60 and ZnPc:PC70BM binary BHJ and ZnPc:rubrene:PC70BM ternary BHJ were deposited as thin films on various substrates. The preservation of the chemical structure of the organic compounds during the MAPLE deposition was confirmed by infrared spectroscopy. The structural, optical, and morphological properties of the deposited layers were investigated by X-ray diffraction (XRD), UV-Vis spectroscopy, photoluminescence (PL), field emission scanning electron microscopy (FESEM), and atomic force microscopy (AFM), respectively. Further, the electrical properties of the developed structures based on ZnPc:C60, ZnPc:PC70BM, and ZnPc:rubrene:PC70BM were evaluated. The J-V characteristics of the organic structures, recorded under illumination, show that an increase in the open-circuit voltage (V_{OC}) is achieved in the case of the ternary blend in comparison with that obtained for the binary blends. The results evidenced that MAPLE-deposited thin films containing binary and ternary organic bulk heterojunctions can find applications in the field of photovoltaic devices.

Keywords: MAPLE; zinc phthalocyanine; fullerene C60; PC70BM; rubrene; photovoltaic cell

1. Introduction

During the last few years, organic materials have been considered as viable alternatives to inorganic materials in various applications [1–4]; they have advantages such as an easy fabrication from solution, deposition at a low temperature, and compatibility with plastic substrates, enhancing the possibility of using these organic compounds in large-area printing deposition [4,5]. Thus, organic materials were successfully integrated in the organic photovoltaic cell (OPV) area, with the best reported efficiency being over 18% [6]. Yet, some improvements are still expected and various organic compounds are being intensively studied to accomplish this goal.

The first OPV was fabricated with a single organic layer with a p-type conduction [7]. An improvement in the cell efficiency was obtained by fabricating OPV with two layers, characterized by different conduction types [8]. A step forward in this domain was achieved by the implementation of the bulk heterojunction (BHJ) concept due to the appearance of the bicontinuous phase separation between the constituent materials [9].

In the fabrication of the OPV structure, the p-type materials which assure light absorption play an important role. From these materials, metallic phthalocyanines (MPc) show a great potential because of their absorption, which covers a broad region of the visible domain of the solar spectrum. Zinc phthalocyanine (ZnPc) is the most used MPc in the OPV, because, besides its specific absorption properties, this MPc is featured by a higher mobility in comparison with other similar compounds [10,11].

In order to form a heterojunction in OPV structures, an n-type material must be mixed with a p-type material. Due to its mobility, C60 fullerene is frequently used as acceptor component in the OPV. However, the low solubility of C60 hinders its deposition from solutions as thin films. For this reason, many attempts have been made to replace C60 with other fullerene derivative compounds with a better solubility, such as [6,6]-phenyl C71 butyric acid methyl ester (PC70BM) [12–14], this compound being widely used in solution-processed electronics. In comparison with other fullerene compounds, PC70BM has also a broader absorption in the visible range of the solar spectrum, and can generate a larger number of excitons in the heterojunction [15], which further dissociates in free charge carriers, resulting in an improvement in the electrical properties of OPV structures.

Among organic semiconductors, 5,6,11,12-tetraphenylnaphthacene (rubrene), a molecule featuring a long exciton-diffusion length, has attracted considerable attention due to its high charge mobility, finding applications in organic electronic devices [16,17].

Lately, various studies have reported an improvement in OPV electrical parameters such as open-circuit voltage (V_{OC}), short-circuit current density (J_{SC}), and fill factor (FF), using ternary blends based on two donors and one acceptor (D1:D2:A), or one donor and two acceptor (D:A1:A2) organic materials compared with binary blends based on one donor and one acceptor (D:A) [18,19]. In this way, involving the same fabrication process for the active layer, a better light harvesting is achieved. Moreover, the V_{OC} value can be increased by forming a better alignment between the highest occupied molecular orbital (HOMO) and the lowest unoccupied molecular orbital (LUMO) of the organic components. Additionally, the electrical parameters can be improved due to a decrease in the trap density, associated with the addition of a third material that can enhance the charge mobility, even in layers with a higher thickness [19].

Although spin-coating is the most common deposition method used in the preparation of a BHJ [13–15], recent reports show the potential of matrix-assisted pulsed-laser evaporation (MAPLE) as an alternative for the deposition of "soft" organic layers. The most important advantages of this laser evaporation technique are (i) that superposed (stacked) layers can be deposited involving the same deposition solvent, and (ii) that a small quantity of the organic material is used in the preparation of the deposition target [12,20–23].

Until now, to our knowledge the growing interest regarding BHJs based on ZnPc:C60 blends was mainly focused on their deposition as thin films by vacuum evaporation [24,25].

In this context, the aim of this study is to fabricate binary and ternary organic BHJs based on ZnPc and fullerene compounds through the MAPLE technique. Thus, ZnPc:C60, ZnPc:PC70BM, and ZnPc:rubrene:PC70BM thin films were deposited and thoroughly characterized to emphasize the influence of the fullerene compound type (C60 or PC70BM) and the addition of a second donor organic material (rubrene) on the electrical parameters of the fabricated photovoltaic structures.

2. Experimental

The organic compounds used for the layer deposition were purchased in powder form as follows: zinc phthalocyanine (ZnPc) and 5,6,11,12-tetraphenylnaphthacene (rubrene) from Sigma-Aldrich (Saint Louis, MO, USA), and C60 fullerene and [6,6]-phenyl C71 butyric acid methyl ester (PC70BM) from Ossila (Sheffield, England). Additionally, poly(3,4-ethylenedioxythiophene) polystyrene sulfonate (PEDOT-PSS) solution and ITO/glass substrates were bought from Ossila, and the dimethyl sulfoxide (DMSO) was purchased from Sigma-Aldrich.

For the preparation of the photovoltaic structures, ITO/glass was used as a transparent conductive oxide substrate. In order to remove the carbon contamination and improve the adherence of the films, this substrate was treated for 10 min in oxygen plasma at 0.6 mbar pressure (Electronic Diener Plasma-Surface-Technology, Pico model equipment, Ebhausen, Germany). Then, the ITO/glass was covered with a thin PEDOT:PSS layer (~40 nm) and deposited by spin-coating at a 6000 rpm speed for 30 sec (Chemat Technology spin coater, KW-4A model, Sigma-Aldrich, Saint Louis, MO, USA), with a thermal annealing process at 120 °C for 5 min being subsequently applied. Furthermore, this substrate was labelled ITO/PEDOT:PSS.

In the MAPLE deposition, an excimer laser source (KrF*, Lambda Physics Coherent, CompexPro 205, λ = 248 nm, τ_{FWHM} ~25 ns, Göttingen, Germany) was used. In this laser deposition process, a frozen target consisting of a solution of an organic compound dissolved in a relatively volatile solvent is irradiated with a laser beam in order to produce a mild vaporization of the target surface. During the deposition, the solvent molecules are pumped away from the deposition chamber by vacuum pumps, with only the organic material molecules reaching the substrate surface and forming organic thin films [12,20]. In Scheme 1, a schematic representation of the experimental set-up used in the MAPLE deposition is presented.

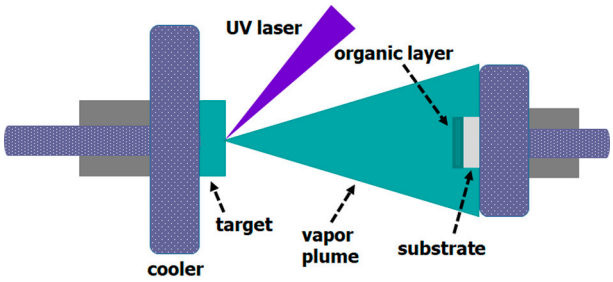

Scheme 1. Schematic representation of the MAPLE set-up used for the deposition of the organic layers.

Before each deposition, the frozen targets were formed from the organic materials dissolved in DMSO, with the total concentration kept at 3% *w*/*v*. Equal proportions of each material (ZnPc, C60, PC70BM, and rubrene) were implied in the binary (1:1) and ternary (1:1:1) mixtures. A low laser fluence (300 mJ/cm^2) was used to prevent the decomposition of the raw materials. The other deposition parameters were kept constant for all the depositions (4×10^{-4} mbar background pressure, 5 cm target–substrate distance, and 10 Hz laser frequency), with only the number of pulses being different (50 K for ZnPc and 100 K for binary and ternary mixtures, respectively). In the same deposition cycle, the organic layers based on ZnPc, ZnPc:C60, ZnPc:PC70BM, and ZnPc:rubrene:PC70BM were deposited on different substrates: ITO/PEDOT:PSS, glass, and silicon. The investigated samples were labelled as follows: ZnPc as a single component (ZnPc), ZnPc:C60 mixture (P1), ZnPc:PC70BM mixture (P2), and ZnPc:rubrene:PC70BM (P3). Their composition, the ratio between their components, and the number of laser pulses used in the deposition of each organic layer are given in Table 1.

Table 1. Organic layers deposited by MAPLE, their composition, the ratio between their components, and the number of laser pulses used in the deposition of each organic layer.

Sample	Composition	Ratio	Number of the Laser Pulses
P0	ZnPc	1	50 K
P1	ZnPc:C60	1:1	100 K
P2	ZnPc:PC70BM	1:1	100 K
P3	ZnPc:rubrene:PC70BM	1:1:1	100 K

The thickness of the deposited layers was estimated using an Ambios Technology XP 100 profilometer (Santa Cruz, CA, USA). Three measurements were carried out for each sample, with the arithmetic media of the obtained values being considered the thickness of the layer as follows: 105 nm for ZnPc, 300 nm for P1, 180 nm for P2, and 285 nm for P3.

The vibrational and structural properties of the deposited thin films were investigated by Fourier transformed infrared spectroscopy (FTIR) and X-ray diffraction (XRD) using a Shimadzu 8400 Spectrometer (Kyoto, Japan) and Bruker D8 Advances equipment (Karlsruhe, Germany) in a Bragg–Bretano geometry with Cu $K_{\alpha 1}$ (λ = 1.4506 Å) monochromatized radiation, respectively. The FTIR spectra were recorded in the 500–1900 cm^{-1} range, while the diffractograms were collected in the 5°–40° domain with a 0.04° step size and 2.5 s/step.

The optical properties of the prepared organic layers were analyzed by UV-VIS spectroscopy and photoluminescence (PL) involving a Thermo Scientific Evolution 220 Spectrophotometer (Waltham, MA, USA) and a FL920 Edinburgh Instruments Spectrometer (Livingston, UK) with a 450 W Xe lamp excitation and double monochromators on both excitation and emission, respectively. The UV-Vis and PL spectra were acquired in the 300–800 nm domain and 450–850 nm range (at a 435 nm excitation wavelength), respectively.

The morphological properties of the MAPLE-deposited layers were investigated by field-emission scanning-electron microscopy (FESEM) and atomic force microscopy (AFM) using a Zeiss Merlin Compact field emission microscope (Oberkochen, Germany) and Nanonics Multiview 4000 system (Jerusalem, Israel), respectively. Additionally, optical images of the organic thin films were acquired using the same system implied in the AFM measurements.

In order to perform the electrical measurements, aluminium (Al), a widely used metal as a contact in the organic heterostructure [26], was deposited as a top contact (100 nm) on a Tectra System (2×10^{-6} mbar, 300 W) by thermal vacuum evaporation. The I-V characteristics of the photovoltaic structures were recorded at room temperature, under AM 1.5 illumination, using an LOT-Oriel solar simulator coupled with a Keithley 2602B System Source Meter (Cleveland, OH, USA).

3. Results and Discussions

The chemical structures of the raw organic materials can be affected during their deposition as organic layers by a laser technique. Infrared spectroscopy is a valuable tool for evaluating the preservation or damage of a chemical structure by revealing the vibrational signatures of the raw organic compounds in the MAPLE-deposited layers. Thus, the FTIR spectra of the MAPLE-deposited thin films from Figure 1a show the specific vibrations of each used organic compound.

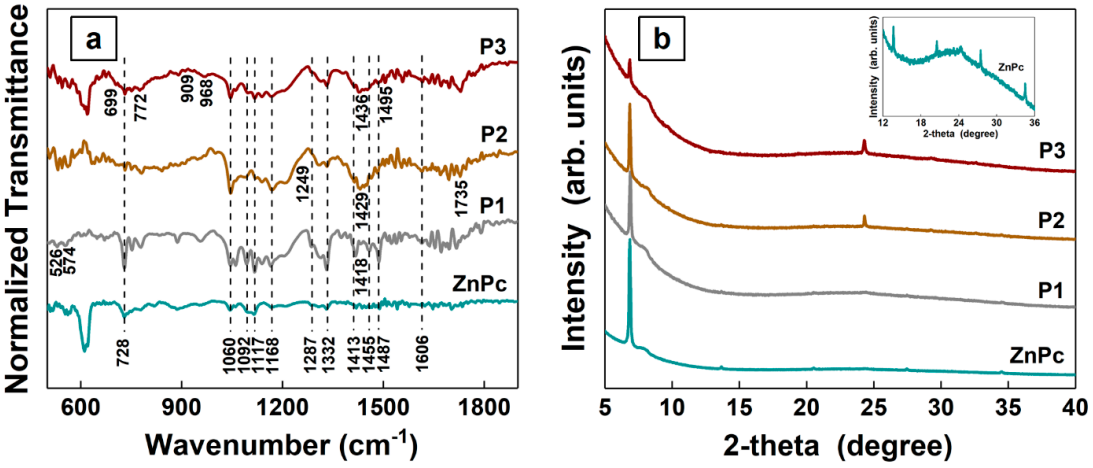

Figure 1. FTIR spectra (**a**) and XRD patterns (**b**) of the MAPLE-deposited organic layers on silicon (**a**) and glass (**b**).

The characteristic peaks of ZnPc can be observed in the FTIR spectra of all the investigated samples, their position being at about: 728 cm^{-1} for C–H bend (out of plane); 1060 and 1168 cm^{-1} for C–H bend; 1092, 1117, and 1287 cm^{-1} for C–H bend (in plane); 1332 cm^{-1} for pyrrole stretch (in plane); 1413 and 1455 cm^{-1} for isoindole stretch; 1487 and 1606 cm^{-1} for C=C benzene stretch [27]. Along with the vibrations attributed to ZnPc, in the FTIR spectra of the P1, P2, and P3 samples the specific features of the other organic components can be also identified as follows: (i) the peaks at about 526, 574, and 1418 cm^{-1} are associated with C60 [28]; (ii) the peaks at about 1429 and 1735 cm^{-1} are correlated with PC70BM [29]; (iii) the peaks at about 699 and 772 cm^{-1} are for C–H bend (out of plane), at 909 and 968 cm^{-1} are C–H bend (out of plane), and at 1436 and 1495 cm^{-1} are C=C stretch in acyl backbone benzene rings related to rubrene [30]. Consequently, the presence of the vibrational fingerprints of each raw organic compound (ZnPc, C60, PC70BM, and rubrene) in the MAPLE-deposited thin films confirm that their chemical structures are preserved, with no chemical decomposition effects taking place during the MAPLE transfer.

The XRD patterns of the MAPLE-deposited thin films given in Figure 1b clearly evidence an intense peak at about 7°, characteristic for ZnPc in thin-film form [31]. The other peaks linked to ZnPc can be barely noticed due to their reduced intensity, at about 13.8°, 20.5°, 27.5°, and 34.5° (PDF 00-011-0714). These results suggest that the organic layers deposited by MAPLE feature a certain crystallinity. In the case of the P2 and P3 samples, the diffractograms disclose a peak at about 24°, which can be related to the presence of PC70BM [32].

The UV-Vis spectra and PL spectra of the MAPLE-deposited thin films are shown in Figure 2a,b, respectively. The UV-Vis spectra of all the deposited films reveal, in the visible region of the solar spectrum, the typical absorption band of the phthalocyanines and the Q band with the Davydov split consisting of a main maximum at ~690 nm and a shoulder at ~640 nm [33]. As regards the weak shoulder which appears at about ~730 nm, this was evidenced in a recent study, being considered as a sub-band of the Q band, with its intensity increasing after an annealing treatment of the ZnPc films at ~150 °C [33]. The other characteristic absorption band of the phthalocyanines, the B (Soret) band peaking at ~360 nm, can be clearly identified in the UV-Vis spectrum of ZnPc, indicating the presence of monomers. The B and Q absorption bands are due to the π-π^* transition having a dipole moment in the molecule plane [24,31,33]. In the case of the P1 sample, the absorption band peaking at ~335 nm is related to the presence of C60 [34]. Besides this, the addition of fullerene compounds induces the following modifications in the absorption of ZnPc: (i) the absorption shoulder peaking at ~640 nm linked to the dimers in phthalocyanines [31] is blue-shifted by the presence of C60 and red-shifted by the presence of PC70BM; (ii) the absorption shoulder peaking at ~730 nm is increased by the presence of PC70BM. Still, due to the ZnPc absorption, the specific bands peaking at ~380 and ~480 nm are associated with PC70BM [35], and those peaking at ~460, ~500, and ~550 nm [36], attributed to rubrene, are not observed in the UV-Vis spectra of the organic blends.

The PL spectra of all the organic layers were analyzed in order to obtain data regarding the charge generation efficiency, information useful in the case of photovoltaic structures. For this reason, the PL measurements were carried on films deposited on ITO/PEDOT:PSS, this substrate being used in the fabrication of the structures investigated by electrical measurements. Regarding the emission of ITO/PEDOT:PSS substrate, the PL spectrum discloses an intense and narrow band centered at ~530 nm and a weak and broad band with two components peaking at ~650 and ~690 nm. As can be seen, the PL spectra of all the investigated samples were dominated by the emission band peaking at ~530 nm due to the ITO/PEDOT:PSS substrate, and the weak and broad emission band characteristics for each organic compounds peaked at ~730 nm for ZnPc [37], ~750 nm for C60 [38], ~710 nm for PC70BM [39], and ~630 nm for rubrene [40] being barely noticed. In the case of binary and ternary mixtures, the PL spectra evidence a quenching effect, with the intensity of the emission bands situated at wavelengths longer than 600 nm being slightly lower in comparison with those of the ZnPc film. Thus, it can be assumed that a slightly smaller part of the charge carrier recombined after the exciton dissociation.

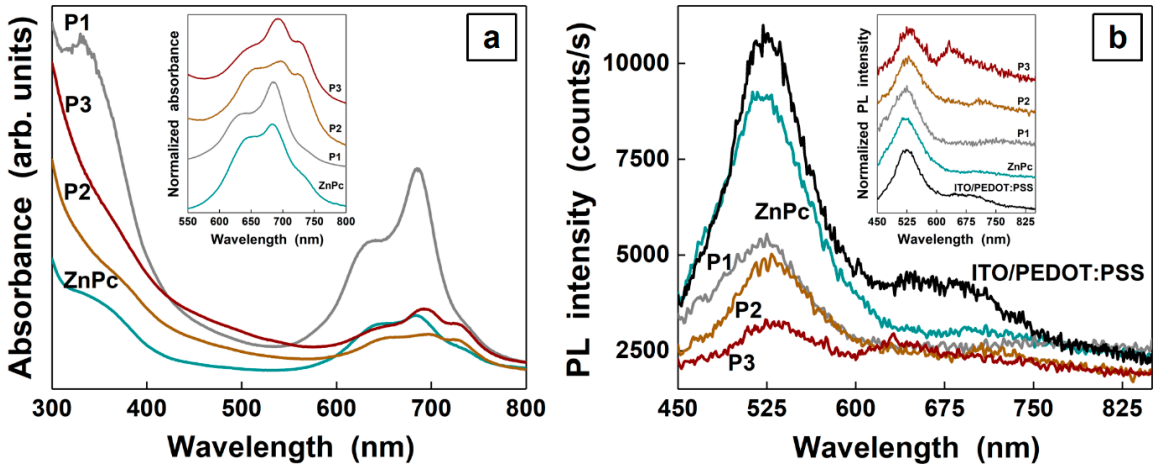

Figure 2. UV-Vis spectra (**a**) and PL spectra (**b**) of the MAPLE-deposited organic layers on glass (**a**) and ITO/PEDOT:PSS (**b**).

The morphology of the active layer is another important parameter in the fabrication of organic photovoltaic structures, with the presence of grain boundaries influencing the charge carrier transport. Thus, the optical, FESEM, and AFM images of the MAPLE-deposited thin films are presented in Figures 3–5, respectively.

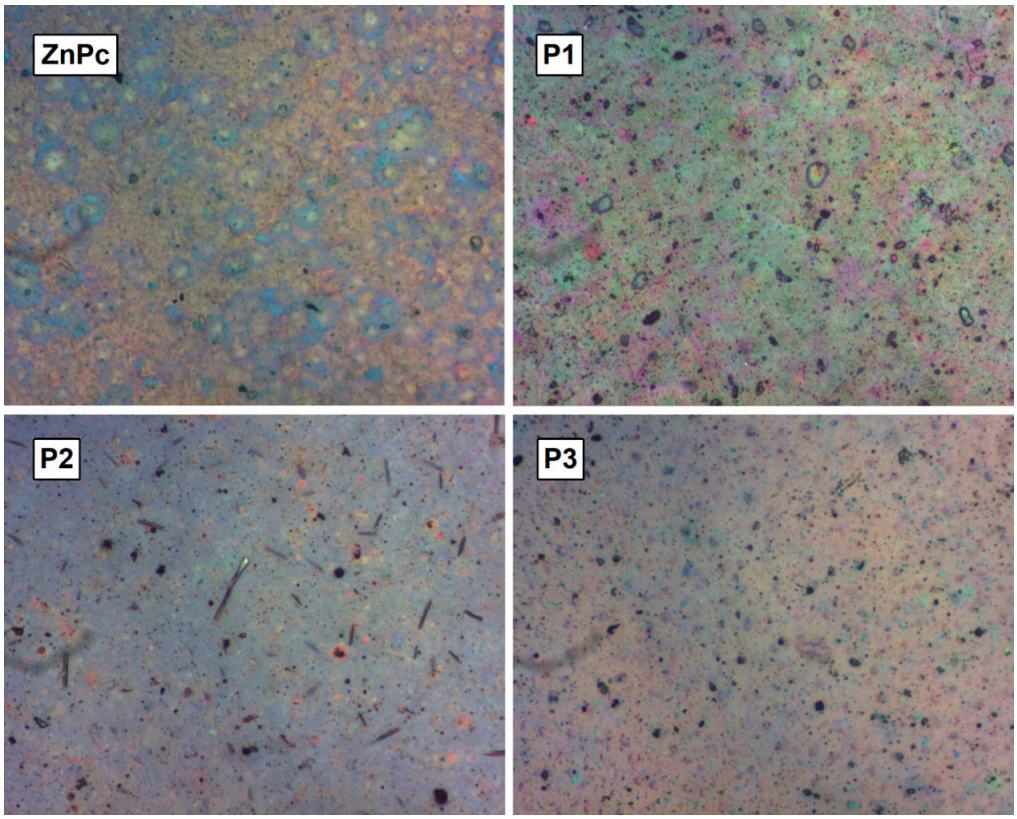

Figure 3. Optical images of the MAPLE-deposited organic layers on glass (500 × 150 × 120 μm^3).

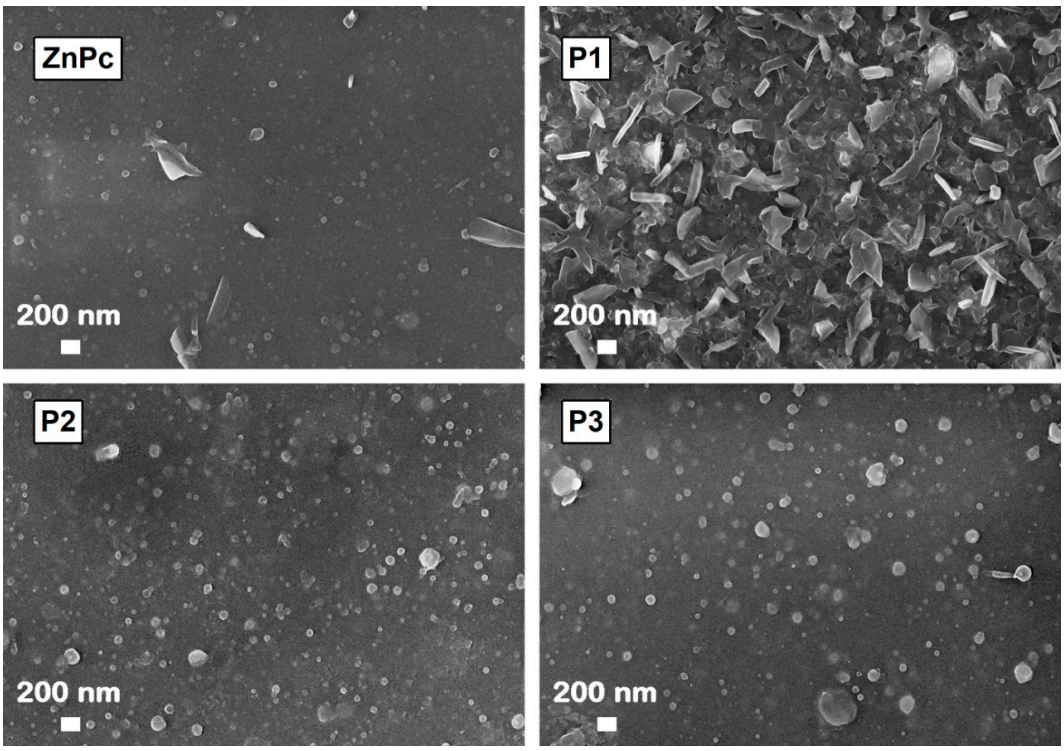

Figure 4. FESEM images of the MAPLE-deposited organic layers on silicon.

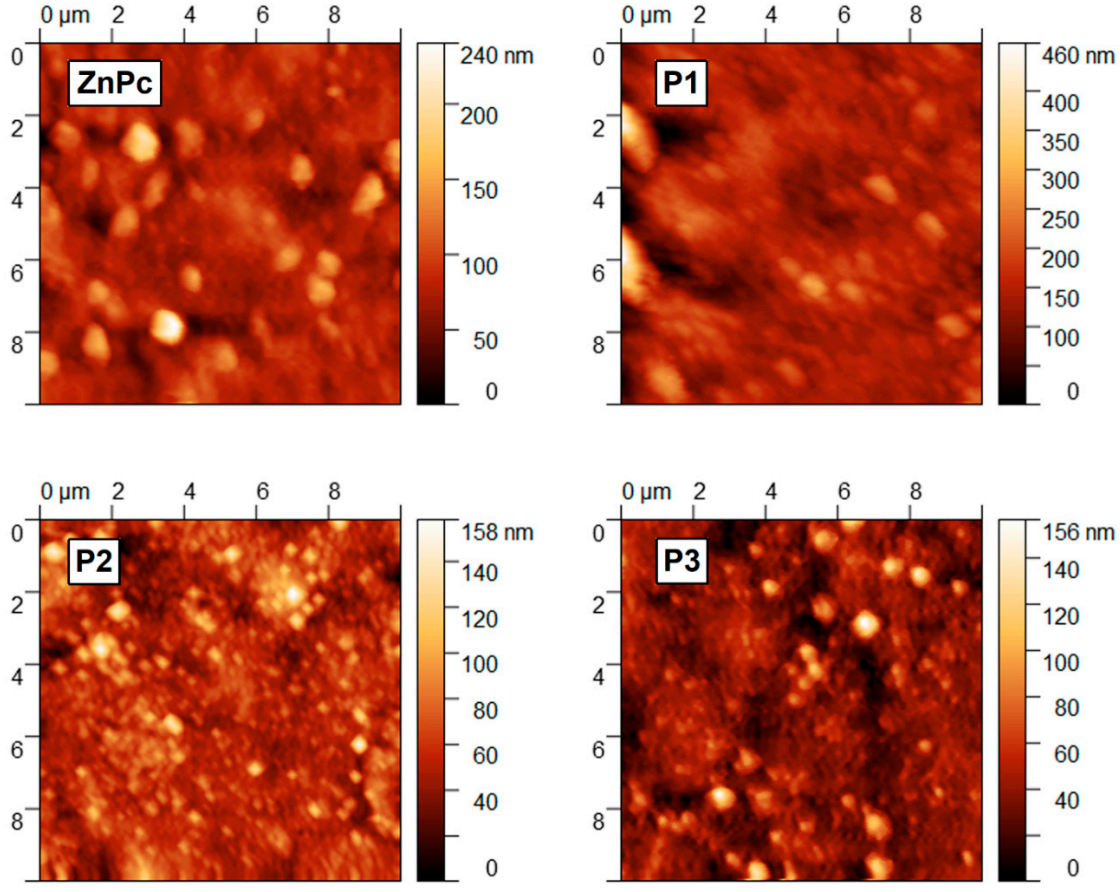

Figure 5. AFM images of the of the MAPLE-deposited organic layers on ITO/PEDOT:PSS.

On a large scale, the optical images (Figure 3) show that the surface of the prepared organic layers is uniform with droplets, this being the specific morphology of the films deposited by MAPLE. Additionally, all the investigated films display an agglomeration process, the effect being more pronounced in the layers based on the binary and ternary mixtures, most probably due to the low solubility of the C60 and rubrene. The FESEM images (Figure 4) reveal a globular morphology for the ZnPc, P2, and P3 samples and a splinter-like morphology for the P1 sample. The roughness parameters (RMS/Ra) were evaluated from the AFM images (Figure 5) as being 22/16 nm for the ZnPc sample, 39/27 nm for the P1 sample, 18/14 nm for the P2 sample, and 30/17 nm for the P3 sample. The ZnPc layer is characterized by large grains, a morphology typical for the films deposited by MAPLE, but also for ZnPc films deposited by other methods [21,41]. Concerning the higher roughness obtained in the case of the P1 sample, this can be explained by taking into account the lower solubility of the C60 compared to PC70BM, the splinter-like morphology, and the thickness of the layer. The roughness of the P2 sample is close to that of the ZnPc layer. As was expected, the roughness increases in the case of the P3 sample due to the addition of the third organic component, rubrene.

The J-V characteristics, recorded under illumination, of the structures developed on the organic bulk heterojunction obtained by MAPLE and a schematic energy level diagram of the materials used in their fabrication are presented in Figure 6a,b, respectively.

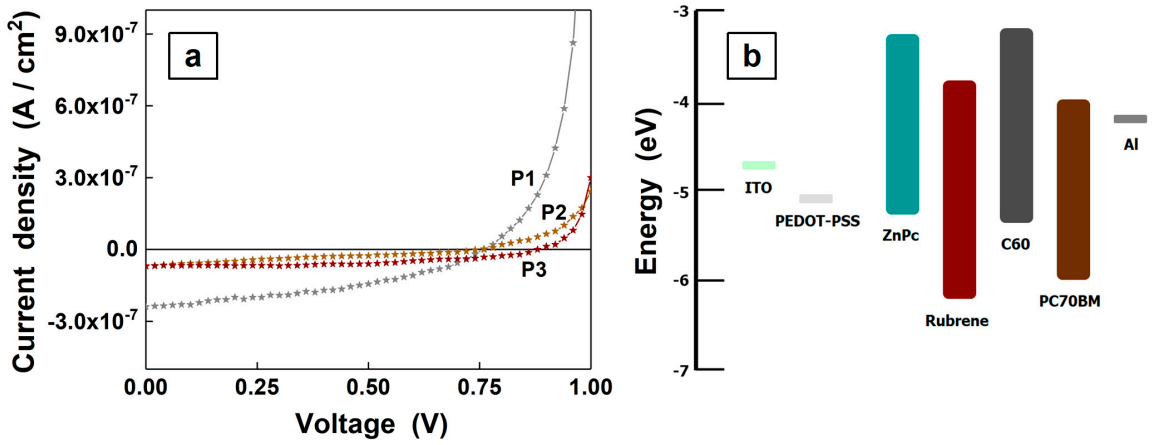

Figure 6. J-V characteristic of the structures based on MAPLE-deposited organic layers on ITO/PEDOT:PSS (**a**) and the energy level diagram of the materials integrated in these structures (**b**).

Additionally, the values of the electrical parameters, short-circuit current density (J_{SC}), open-circuit voltage (V_{OC}), and maximum power (P_{max}) corresponding to each investigated structure are given in Table 2.

Table 2. Electrical parameters of the MAPLE-deposited organic layers.

Sample	V_{OC} [V]	J_{SC} [A]	P_{max} [W]
P1	0.76	2.4×10^{-7}	5.6×10^{-8}
P2	0.74	6.9×10^{-8}	1.2×10^{-8}
P3	0.88	6.9×10^{-8}	3.1×10^{-8}

Thus, the P1 and P2 samples containing a mixture between ZnPc and C60 or ZnPc and PC70BM present a very small variation in the V_{OC} value. Moreover, the P1 sample shows the highest J_{SC} value (2.4×10^{-7} A). The result can be explained taking into account the following aspects: (i) the higher absorption of the layer containing C60, a larger quantity of light being absorbed in the active area leading to the highest value of J_{SC} and (ii) the small difference between the LUMO orbitals of C60 and ZnPc (ΔE = 0.4 eV, $E_{LUMO,C60}$ = 3.7 eV, $E_{LUMO,ZnPc}$ = 3.3 eV [21,42]) compared with those of PC70BM

and ZnPc (ΔE = 0.7 eV, $E_{LUMO,PC70BM}$ = 4 eV [43]). Even if the P2 and P3 samples are characterized by the same J_{SC} value, the addition of rubrene in the mixture containing ZnPc and PC70BM results in an increase in the V_{OC} parameter from 0.74 V (P2 sample) at 0.88 V (P3 sample). A similar result was observed in the case of photovoltaic structures fabricated with other binary and ternary layers [18,19]. The increase in the V_{OC} parameter is linked to a better energy alignment (cascade) between the organic compounds, with the HOMO level of the D2 lower than that of the D1; in our case, the HOMO orbitals of rubrene ($E_{HOMO,rubrene}$ = 5.4 eV [1]) and ZnPc ($E_{HOMO,ZnPc}$ = 5.2 eV [19]), respectively. Additionally, all the samples show similar values of P_{max}.

Although the J_{SC} parameter in the fabricated structures is not higher due to the non-radiative quenching of the excitons effects and to the roughness parameters which can affect the percolation path of the charge carrier toward electrodes [25], it can be improved by using a higher concentration of the organic compounds than that involved in this work (3% *w*/*v*) in the MAPLE process. Thus, by increasing the concentration of the organic components in the MAPLE target, the absorption of the deposited films will be enhanced, leading to an increase in the number of the generated excitons which will dissociate in a larger number of free charge carriers, resulting finally in an improvement in the electrical parameters of the organic structure. Additionally, a recent study focusing on the RIR-MAPLE deposition of the conjugated polymers [44] evidences that the improvement of the J_{SC} parameter can be achieved by involving, during the MAPLE process, a solvent which allows the deposition of organic films with a lower roughness. Consequently, the outcome of this work is promising for future studies focused on ternary organic cell structures obtained by the MAPLE technique.

4. Conclusions

Thin films based on ZnPc, ZnPc:C60, ZnPc:PC70BM, and ZnPc:rubrene:PC70BM were deposited by MAPLE, being further used as active layers in binary and ternary organic solar cell structures. The FTIR spectra confirm that the chemical structure of organic components, such as ZnPc, C60, PC70BM, and rubrene, is preserved during the laser evaporation process. In the UV-Vis spectra of the MAPLE-deposited layers the typical absorption band of ZnPc prevails, while their PL spectra are dominated by the emission linked to the ITO/PEDOT:PSS substrate, with the emission bands characteristic of each organic compound (ZnPc, C60, PC70BM, rubrene) being barely identified. The morphological investigations reveal a globular morphology for the ZnPc, ZnPc:PC70BM, and ZnPc:rubrene:PC70BM samples and a splinter-like morphology for the ZnPc:C60 sample. The J-V characteristics of the organic structures recorded under illumination show that an increase in the open-circuit voltage (V_{OC}) is achieved in the case of the ternary blend in comparison with that obtained for binary blends, while the value of the short-circuit current (J_{SC}) is comparable for the investigated structures. The results emphasize the potential of these structures developed on the MAPLE-deposited thin films containing binary and ternary organic bulk heterojunctions in the field of organic photovoltaic devices.

Author Contributions: M.S.: Conceptualization, Writing—original draft, Investigation. N.P.: Validation, Writing—review and editing, Investigation. G.P.: Investigations. A.C.: Investigations. Writing—original draft. O.R.: Investigations. G.P.-P.: Investigation. A.M.: Investigation. A.S.: Validation, Writing—review and editing, Investigation. G.S.: Supervisor. Investigation, Writing—review and editing. All authors have read and agreed to the published version of the manuscript.

Funding: This research was funded by the Romanian Ministry of Education and Research through National Core Founding Program (PN19-03 -contract no. 21 N/2019 and PN19-15 -contract No. 16 N/2019) and by Project No. 62/2020 (IUCN ORDER No. 269/20.05.2020) of JINR–Romania collaboration (Theme No. 03-4-1128-2017/2022).

Conflicts of Interest: The authors declare no conflict of interest.

References

1. Engmann, S.; Barito, A.J.; Bittle, E.G.; Giebink, N.C.; Richter, L.J.; Gundlach, D.J. Higher order effects in organic LEDs with sub-bandgap turn-on. *Nat. Commun.* **2019**, *10*, 227. [CrossRef] [PubMed]
2. Jazbinsek, M.; Puc, U.; Abina, A.; Zidansek, A. Organic crystals for THz photonics. *Appl. Sci.* **2019**, *9*, 882. [CrossRef]
3. Stanculescu, A.; Stanculescu, F.; Alexandru, H.V.; Socol, M. Doped aromatic derivatives wide-gap crystalline semiconductor structured layers for electronic applications. *Thin Solid Films* **2006**, *495*, 389–393. [CrossRef]
4. Gusain, A.; Faria, R.M.; Miranda, P.B. Polymer solar cells—Interfacial processes related to performance issues. *Front. Chem.* **2019**, *7*, 61. [CrossRef] [PubMed]
5. Chang, J.; Sonar, P.; Lin, Z.; Zhang, C.; Zhang, J.; Hao, Y.; Wu, J. Controlling aggregation and crystallization of solution processed diketopyrrolopyrrole based polymer for high performance thin film transistors by pre-metered slot die coating process. *Org. Electron.* **2016**, *36*, 113–119. [CrossRef]
6. Liu, Q.; Jiang, Y.; Jin, K.; Qin, J.; Xu, J.; Li, W.; Xiong, J.; Liu, J.; Xiao, Z.; Sun, K.; et al. 18% Efficiency organic solar cells. *Sci. Bull.* **2020**, *65*, 272–275. [CrossRef]
7. Kearns, D.; Calvin, M. Photovoltaic effect and photoconductivity in laminated organic systems. *J. Chem. Phys.* **1958**, *29*, 950–951. [CrossRef]
8. Tang, C.W. Two-layer organic photovoltaic cell. *Appl. Phys. Lett.* **1986**, *48*, 183–185. [CrossRef]
9. Yu, G.; Gao, J.; Hummelen, J.C.; Wudl, F.; Heeger, A.J. Polymer photovoltaic cells: Enhanced efficiencies via a network of internal donor-acceptor heterojunctions. *Science* **1995**, *270*, 1789–1791. [CrossRef]
10. Islam, Z.U.; Tahir, M.; Syed, W.A.; Aziz, F.; Wahab, F.; Said, S.M.; Sarker, R.M.; Md Ali, S.H.; Sabri, M.F.M. Fabrication and photovoltaic properties of organic solar cell based on zinc phthalocyanine. *Energies* **2020**, *13*, 962. [CrossRef]
11. Jiang, H.; Hu, P.; Ye, J.; Ganguly, R.; Li, Y.; Long, Y.; Fichou, D.; Hu, W.; Kloc, C. Hole mobility modulation in single–crystal metal phthalocyanines by changing the metal–π/π–π interactions. *Angew. Chem. Int. Ed.* **2018**, *57*, 10112–10117. [CrossRef] [PubMed]
12. Stanculescu, F.; Rasoga, O.; Catargiu, A.M.; Vacareanu, L.; Socol, M.; Breazu, C.; Preda, N.; Socol, G.; Stanculescu, A. MAPLE prepared heterostructures with arylene based polymer active layer for photovoltaic applications. *Appl. Surf. Sci.* **2015**, *336*, 240–248. [CrossRef]
13. Armin, A.; Hambsch, M.; Wolfer, P.; Jin, H.; Li, J.; Shi, Z.; Burn, P.L.; Meredith, P. Efficient, large area, and thick junction polymer solar cells with balanced mobilities and low defect densities. *Adv. Energy Mater.* **2014**, *5*, 1401221. [CrossRef]
14. Armin, A.; Wolfer, P.; Shaw, P.E.; Hambsch, M.; Maasoumi, F.; Ullah, M.; Gann, E.; McNeill, C.R.; Li, J.; Shi, Z.; et al. Simultaneous enhancement of charge generation quantum yield and carrier transport in organic solar cells. *J. Mater. Chem. C* **2015**, *41*, 10799–10812. [CrossRef]
15. Zhang, F.; Zhuo, Z.; Zhang, J.; Wang, X.; Xu, X.; Wang, Z.; Xin, Y.; Wang, J.; Wang, J.; Tang, W.; et al. Influence of PC60BM or PC70BM as electron acceptor on the performance of polymer solar cells. *Sol. Energy Mater. Sol. Cells.* **2012**, *97*, 71–77. [CrossRef]
16. Pandey, A. Highly efficient spin-conversion effect leading to energy up-converted electroluminescence in singlet fission photovoltaics. *Sci. Rep.* **2015**, *5*, 7787. [CrossRef]
17. Hasegawa, T.; Takeya, J. Organic field-effect transistors using single crystals. *Sci. Technol. Adv. Mater.* **2009**, *10*, 024314. [CrossRef]
18. Dayneko, S.V.; Hendsbee, A.D.; Cann, J.R.; Cabanetos, C.; Welch, G.C. Ternary organic solar cells: Using molecular donor or acceptor third components to increase open circuit voltage. *New J. Chem.* **2019**, *43*, 10442–10448. [CrossRef]
19. Gasparini, N.; Salleo, A.; McCulloch, I.; Baran, D. The role of the third component in ternary organic solar cells. *Nat. Rev. Mater.* **2019**, *4*, 229–242. [CrossRef]
20. Caricato, A.P.; Cesaria, M.; Gigli, G.; Loiudice, A.; Luches, A.; Martino, M.; Resta, V.; Rizzo, A.; Taurino, A. Poly-(3-hexylthiophene)/[6,6]-phenyl-C61-butyric-acid-methyl-ester bilayer deposition by matrix-assisted pulsed laser evaporation for organic photovoltaic applications. *Appl. Phys. Lett.* **2012**, *100*, 073306. [CrossRef]
21. Socol, M.; Preda, N.; Rasoga, O.; Breazu, C.; Stavarache, I.; Stanculescu, F.; Socol, G.; Gherendi, F.; Grumezescu, V.; Stefan, N.; et al. Flexible heterostructures based on metal phthalocyanines thin films obtained by MAPLE. *Appl. Surf. Sci.* **2016**, *374*, 403–410. [CrossRef]

22. Ionita, I.; Bercea, A.; Brajnicov, S.; Matei, A.; Ion, V.; Marascu, V.; Mitu, B.; Constantinescu, C. Second harmonic generation (SHG) in pentacene thin films grown by matrix assisted pulsed laser evaporation (MAPLE). *Appl. Surf. Sci.* **2019**, *480*, 212–218. [CrossRef]
23. Stanculescu, A.; Rasoga, O.; Mihut, L.; Socol, M.; Stanculescu, F.; Ionita, I.; Albu, A.-M.; Socol, G. Preparation and characterization of polar aniline functionalized copolymers thin films for optical non-linear applications. *Ferroelectrics* **2009**, *389*, 159–173. [CrossRef]
24. Schunemann, C.; Wynands, D.; Wilde, L.; Hein, M.P.; Pfutzner, S.; Elschner, C.; Eichhorn, K.-J.; Leo, K.; Riede, M. Phase separation analysis of bulk heterojunctions in small-molecule organic solar cells using zinc-phthalocyanine and C60. *Phys. Rev. B* **2012**, *85*, 245314. [CrossRef]
25. Pfuetzner, S.; Meiss, J.; Petrich, A.; Riede, M.; Leo, K. Thick C60: ZnPc bulk heterojunction solar cells with improved performance by film deposition on heated substrates. *Appl. Phys. Lett.* **2009**, *94*, 253303. [CrossRef]
26. Sanculescu, F.; Stanculescu, A.; Socol, M. Effect of the metallic contact on the electrical properties of organic semiconductor film. *J. Optoelectron. Adv. Mater.* **2007**, *9*, 1352–1357.
27. Gaffo, L.; Cordeiro, M.R.; Freitas, A.R.; Moreira, W.C.; Girotto, E.M.; Zucolotto, V. The effects of temperature on the molecular orientation of zinc phthalocyanine films. *J. Mater. Sci.* **2010**, *45*, 1366–1370. [CrossRef]
28. Pu, J.; Mo, Y.; Wan, S.; Wang, L. Fabrication of novel graphene–fullerene hybrid lubricating films based on self-assembly for MEMS applications. *Chem. Commun.* **2014**, *50*, 469–471. [CrossRef]
29. Blazinic, V.; Ericsson, L.K.; Muntean, S.A.; Moons, E. Photo-degradation in air of spin-coated PC60BM and PC70BM films. *Synth. Met.* **2018**, *241*, 26–30. [CrossRef]
30. Gavrilko, T.; Nechytaylo, V.; Viduta, L.; Baran, J. Optical properties and stability of bilayer rubrene-Alq3 films fabricated by vacuum deposition. *Ukr. J. Phys.* **2018**, *63*, 362. [CrossRef]
31. Zanfolim, A.A.; Volpati, D.; Olivati, C.A.; Job, A.E.; Constantino, C.J.L. Structural and electric-optical properties of zinc phthalocyanine evaporated thin films: Temperature and thickness effects. *J. Phys. Chem. C* **2010**, *114*, 12290–12299. [CrossRef]
32. Viterisi, A.; Montcada, N.F.; Kumar, C.V.; Guirado, F.G.; Martin, E.; Escuderoa, E.; Palomares, E. Unambiguous determination of molecular packing in crystalline donor domains of small molecule solution processed solar cell devices using routine X-ray diffraction techniques. *J. Mater. Chem. A* **2014**, *2*, 3536–3542. [CrossRef]
33. Ahn, H.; Chu, T.-C. Annealing-induced phase transition in zinc phthalocyanine ultrathin films. *Opt. Mater. Express* **2016**, *6*, 3587. [CrossRef]
34. Peng, Y.; Zhang, L.; Chengand, N.; Andrew, T. ITO-free transparent organic solar cell with distributed bragg reflector for solar harvesting windows. *Energies* **2017**, *10*, 707. [CrossRef]
35. Hou, J.; Guo, X. Active layer materials for organic solar cells. In *Organic Solar Cells. Green Energy and Technology*, 1st ed.; Choy, W., Ed.; Springer: London, UK, 2013; pp. 17–42.
36. Zhang, X.; Wu, Z.; Jiao, B.; Wang, D.; Wang, D.; Hou, X.; Huang, W. Solution-processed white organic light-emitting diodes with mixed-host structures. *J. Lumin.* **2012**, *132*, 697–701. [CrossRef]
37. Zafar, Q.; Fatima, N.; Karimov, K.S.; Ahmed, M.M.; Sulaiman, K. Realizing broad-bandwidth visible wavelength photodiode based on solution-processed ZnPc/PC71BM dyad. *Opt. Mater.* **2017**, *64*, 131–136. [CrossRef]
38. Elistratova, M.A.; Zakharova, I.B.; Romanov, N.M. Obtaining and investigation of C_{60} <A_2B_6> semiconductor compounds with a view to create effective solar cells. *J. Phys. Conf. Ser.* **2015**, *661*, 012030. [CrossRef]
39. Griffin, J.; Pearson, A.J.; Scarratt, N.W.; Wang, T.; Dunbar, A.D.F.; Yi, H.; Iraqi, A.; Buckley, A.R.; Lidzey, D.G. Organic photovoltaic devices with enhanced efficiency processed from non-halogenated binary solvent blends. *Org. Electron.* **2015**, *21*, 216–222. [CrossRef]
40. Liang, C.; Jin-Xiang, D.; Le, K.; Min, C.; Ren-Gang, C.; Zi-Jia, Z. Optical properties of rubrene thin film prepared by thermal evaporation. *Chin. Phys. B* **2015**, *24*, 047801.
41. Klyamer, D.D.; Sukhikh, A.S.; Gromilov, S.A.; Kruchinin, V.N.; Spesivtsev, E.V.; Hassan, A.K.; Basova, T.V. Influence of fluorosubstitution on the structure of zinc phthalocyanine thin films. *Macroheterocycles* **2018**, *11*, 304–311. [CrossRef]
42. Lassiter, B.E.; Wei, G.; Wang, S.; Zimmerman, J.D.; Diev, V.V.; Thompson, M.E.; Forrest, S.R. Organic photovoltaics incorporating electron conducting exciton blocking layers. *Appl. Phys. Lett.* **2011**, *98*, 243307. [CrossRef]

43. Singh, R.; Suranagi, S.R.; Lee, J.; Lee, H.; Kim, M.; Cho, K. Unravelling the efficiency-limiting morphological issues of the perylene diimide-based nonfullerene organic solar cells. *Sci. Rep.* **2018**, *8*, 2849. [CrossRef] [PubMed]
44. Ge, W.; Li, N.K.; McCormick, R.D.; Lichtenberg, E.; Yingling, Y.G.; Stiff-Robers, A.D. Emulsion-based RIR-MAPLE deposition of conjugated polymers: Primary solvent effect and its implications on organic solar cell performance. *ACS Appl. Mater. Interfaces* **2016**, *8*, 19494–19506. [CrossRef] [PubMed]